The Formation of Gold Clusters Supported on Mesoporous Silica Material Surfaces: A Molecular Picture

4 AUTHORS, INCLUDING:

Anna Wojtaszek
Adam Mickiewicz University
9 PUBLICATIONS   99 CITATIONS

SEE PROFILE

Maria Ziolek
Adam Mickiewicz University
204 PUBLICATIONS   3,435 CITATIONS

SEE PROFILE

Frederik Tielens
Collège de France
93 PUBLICATIONS   1,330 CITATIONS

SEE PROFILE

The Formation of Gold Clusters Supported on Mesoporous Silica Material Surfaces: A Molecular Picture

A. Wojtaszek,[†,‡,§] I. Sobczak,[§] M. Ziolek,[§] and F. Tielens*[,†,‡]

UPMC Univ Paris 06, UMR 7197, Laboratoire de Réactivité de Surface, Tour 54-55, 2ème étage - Casier 178, 4, Place Jussieu, F-75005 Paris, France, CNRS, UMR 7609, Laboratoire de Réactivité de Surface, Tour 54-55, 2ème étage - Casier 178, 4, Place Jussieu, F-75005 Paris, France, and Adam Mickiewicz University, Faculty of Chemistry, Grunwaldzka 6, 60-780 Poznań, Poland

The interaction of gold particles with a silica surface is investigated using a combination of theoretical and experimental techniques. It is found that the physisorption strength of gold on silica decreases with increasing chloride concentration at the surface, with increasing cluster size, and with decreasing oxidation state of gold. However, the gold precursor is adsorbed more strongly than the corresponding precursor fragments and this via an H-bond network. It is also found that chemisorbed, grafted species may coexist on a silica surface, depending on the experimental conditions. From the vibrational frequencies and especially by the presence of a band at 3650 cm^{-1}, it is found that the gold species after calcination are probably present under the form of digrafted chemisorbed species. This information enables us to propose a scenario for the formation of gold clusters at the silica surface.

Introduction

Ordered mesoporous matrices with high surface areas were intensively studied as supports for gold species. Metallic gold is recognized as the main active species in many redox reactions.[1] The reduction of gold cations occurs at a relatively low temperature and even in air atmosphere.[1,2]

Various parameters, including temperature and atmosphere of activation and reducibility of the support, have been already considered in the chemistry, structure, and catalytic activity of gold-containing solids.[3]

However, many questions remain unanswered considering the molecular structure of the silica-supported gold catalyst.

Recently, we described the very first step of the gold dispersion process at silica surfaces, in which we confirmed the pH dependency of the gold precursor HAuCl$_4$ and the influence of chlorides at the surface on the precursor's adsorption behavior.[4] In the present study, we want to shed some light on the subsequent steps of the formation of gold clusters at a silica surface. For this reason, the precursor fragments AuCl$_n$ and AuOH are investigated, as well as the effect of the size of the gold cluster. Next, to the physisorbed complexes, models for gold chemisorption are proposed. Finally, a possible scenario is presented for the formation of dispersed silica-supported gold catalysts.

In summary, we perform a systematic theoretical and computational study on a series of possible silica-supported gold catalyst surfaces in hydrated and dehydrated forms. The nature of the gold species is investigated from the inspection of final geometry and corresponding total energy. An atomistic thermodynamics approach is then used to bridge the gap between the 0 K calculations and the conditions of temperature and pressure used in the spectroscopic measurements. This allows estimating the predominance of the different species as a function of temperature and hydration conditions. Finally, vibrational spectra are calculated and compared with experimental results in order to assign representative bands and characterize the silica material.

Computational Details

The ordered mesoporous material MCM-41 is modeled using an amorphous hydrated silica slab, designed, described, and characterized by our group.[5] The silica slab consists of more than 120 atoms (Si$_{27}$O$_{54}$·13H$_2$O), which enables modeling a correct representation of a hydrated silica surface. The same model has been used with success in studies concerning the interaction with AuCl$_n$(OH)$_{4-n}^-$,[4] vanadium oxide grafting,[6] and amino acid adsorption.[7,8]

Experimentally, the HAuCl$_4$ molecule is adsorbed on the surface under different forms, depending on the pH of the solution. The gold precursor is dechlorinated forming AuCl$_n$(OH)$_{4-n}^-$ species.[9,10] The adsorption process has been described using periodic DFT in a recent publication.[4] After preparation of the catalyst, no Au^{III} is found on the surface, only metallic Au^0 and Au^I.[2,11,12] The adsorption of gold atoms and clusters is investigated on the same silica surface model as was used for the precursor AuCl$_n$(OH)$_{4-n}^-$.[4] The interaction of Au$_n$Cl$_m$ and Au$_n$(OH)$_m$ species are investigated for odd *n* up to 5 and *m* 0 or 1. *n* is chosen to be odd because of the well-known odd/even behavior of the molecular properties of gold clusters[13] and also to have a closed shell configuration of the chlorinated clusters. The cluster shape of the Au$_3$ and Au$_5$ clusters is chosen to be planar (2D), as is observed in the gas phase,[14] that is, triangular planes (see Figure 1). No other geometries were considered in this study.

On the surface, a silanol nest consisting of three Si−OH groups is chosen as the adsorption site. The Si−OH groups are than substituted by Si−Cl groups in order to introduce the effect of Cl during the cluster formation. In the second part of the study, chemisorbed species are introduced in order to investigate

---

　* To whom correspondence should be addressed. E-mail: frederik.tielens@upmc.fr.
　† UPMC Univ Paris 06, UMR 7197.
　‡ CNRS, UMR 7609.
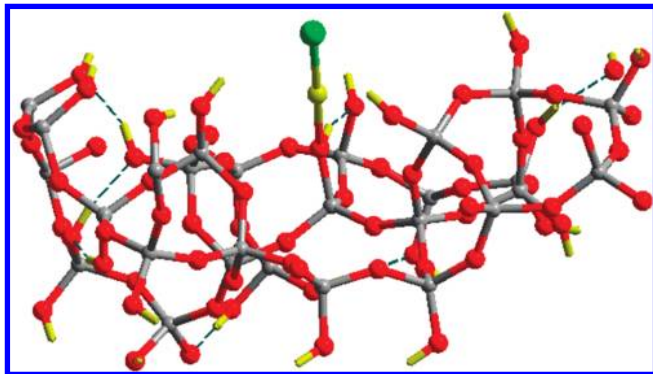　§ Adam Mickiewicz University.

Figure 1. Most stable $Au_n(AuCl)$ physisorption geometry.

TABLE 1: Adsorption Energy for the Different Forms of the Gold Species Studied on the Silica Surface (values in eV)

no. of Cl @ surface	AuCl	Au_3Cl	Au_5Cl	Au^0
0	−1.51	−1.04	−0.66	−0.33
1	−1.06	−0.93	−0.19	0.07
2	−0.81	−0.82	−0.06	−0.01
3	−0.68	−0.90	0.05	0.00

the possible formation of Au−O−Si linkages after calcinations of the material. The stability of the chemisorbed species is investigated as a function of hydration, using first-principles atomistic thermodynamics, an approach successfully used in former studies.[6,15,16]

All calculations are performed using ab initio plane-wave pseudopotential calculations implemented in VASP.[17,18] The Perdew−Burke−Ernzerhof (RPBE) functional[19−21] has been chosen to perform the periodic DFT calculations with an accuracy on the overall convergence tested elsewhere.[22−26] The valence electrons are treated explicitly, and their interactions with the ionic cores are described by the projector augmented-wave method (PAW),[27,28] which allows using a low-energy cutoff equal to 400 eV for the plane-wave basis. The integral over the first Brillouin zone is performed using the gamma point. The positions of all the atoms in the supercell are relaxed, in the potential energy determined by the full quantum mechanical electronic structure until the total energy differences between the loops decrease below 10^{-4} eV.

Vibrational frequencies have been calculated for selected surface species within the harmonic approximation. Only the gold center and its first and second neighbors (O−Si and OH groups) are allowed to move; the support is kept fixed. The Hessian matrix is computed by the finite difference method, followed by a diagonalization procedure. The eigenvalues of the resulting matrix lead to the frequency values. The assignment of the vibrational modes is done by inspection of the corresponding eigenvectors.

FTIR Study

Infrared spectra were recorded with the Vector 22 (Bruker) spectrometer (resolution = 4 cm^{-1}, number of scans = 64). The pressed wafers of the materials (∼5 mg cm^{-1}) were placed in the vacuum cell and evacuated at 623 K for 3 h. The temperature ramp was 10 K/min from RT to 623 K. After evacuation, the spectra of samples were registered at room temperature (RT).

Results

The Effect of the Au Cluster Size on the Adsorption Behavior. Metallic gold atoms are very weakly adsorbed (−0.33 eV) to the silica surface (see Table 1 and Figure 2). The presence of chloride destabilizes the already weak interaction with a gold atom, independent of the amount of chlorides at the surface. Metallic gold atoms do not adsorb on silica if chlorides are present.

Nevertheless, Au^I under the form of AuCl adsorbs with an exothermic energy of −1.51 eV, decreasing with the number of chlorides at the surface. The adsorption of AuOH is found to be unfavorable due to the lower polarization of the Au−OH

bond compared with the Au−Cl bond. The adsorption energy of AuCl on a Si−Cl nest composed of three chlorides is still −0.68 eV. The presence of chloride is, however, unfavorable, but less pronounced, than for metallic gold. The same trend was found for Au^{III} species, but with higher adsorption energies.[4]

When the number of Au atoms is increased to three (Au_3Cl), the adsorption energy decreases slightly but seems to converge with increasing number of chlorides at the silica surface to approximately −0.9 eV. However, for AuCl, the adsorption energy decreases every time an extra chloride is added to the surface. Interestingly, one can note that the triangular Au_3Cl cluster interacts with the surface with a Si−Cl group instead of a silanol group; however, the interaction with a silanol group is stronger when no Si−Cl groups are present in its neighborhood. This behavior indicates that the silanol groups are influenced by the presence of chlorides at the surface. Because the adsorption process is more favorable when there are no chlorides at the surface, the gold species will probably migrate to chloride-free areas on the silica surface.

For planar Au_5Cl clusters, the adsorption decreases with the number of chlorides at the silica surface, but the preference to adsorb on a Si−Cl group occurs only when two Si−Cl groups are close to each other. Otherwise, the silanol groups are the preferred adsorption sites. The geometry of the adsorption site does not permit an interaction through two anchor points because the cluster is too small to interact with an oxygen atom of the silanol group; the chloride group of the Au_5Cl cluster introduces a repulsive interaction between the Cl group and a surface silanol.

Extrapolating these results to Au_7 and larger clusters, one expects that the adsorption energy decreases further, which means that the gold clusters do not interact strongly with the surface. The gold clusters will only be tightly bonded to silica if a chemical bond between Au and a surface oxygen is formed, and this is a consequence of the calcination process. After the calcination process, the system is dehydrated and it is expected that most OH groups leave the gold precursor ($AuCl_n(OH)_{4-n}^-$) and gold reduces from III to I or 0.

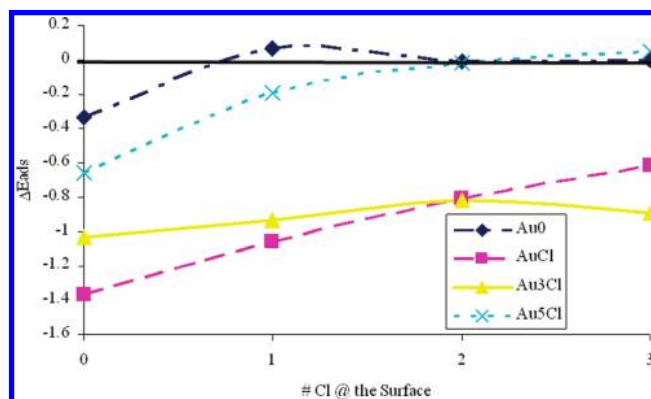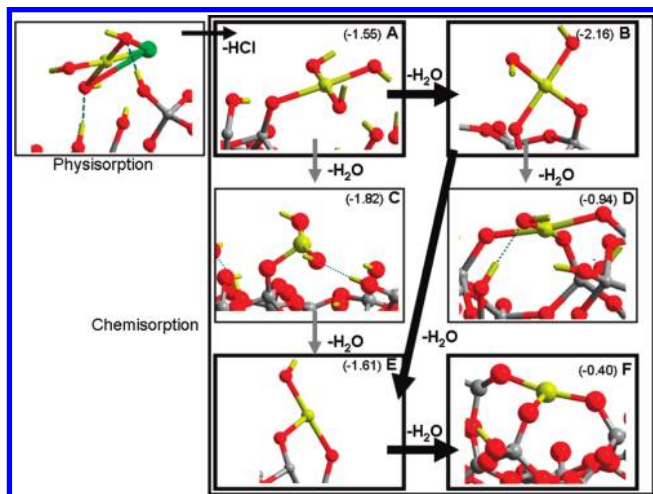Because the adsorption energy decreases with the gold cluster size, gold is expected to form Au−O−Si linkages with the

Figure 2. Adsorption energy for the different gold species calculated on different Cl-containing silica slabs. Values are in eV.
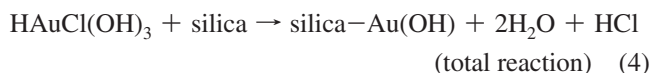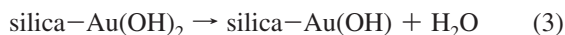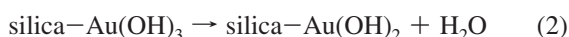
Figure 3. Optimized geometries of gold chemisorbed species on silica. Binding energies (eV) are in parentheses.

surface, and thus, the first step in this process would be the reaction of the adsorbed gold precursor $(AuCl_n(OH)_{4-n}^-)$ with the silica surface.

The Chemisorbed Species. The oxidation state of gold in the $(AuCl_n(OH)_{4-n}^-)$ complex is III. Because it has been shown experimentally and theoretically that the most stable adsorption complex between the gold precursor and the surface is $AuCl(OH)_3^-$, adsorbed on a chloride-free surface,[4] the successive reactions proposed to obtain chemisorbed species are

$$HAuCl(OH)_3 + silica \rightarrow silica-Au(OH)_3 + HCl \quad (1)$$
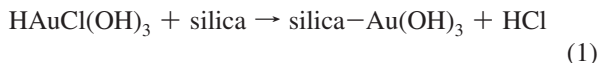
The optimized geometry of the chemisorbed dechlorinated species is shown in Figure 3A. The next step is the formation of two Si-O-Au linkages by dehydration, (see Figure 3B), followed by a subsequent and last dehydration step (see Figure 3D).

$$silica-Au(OH)_3 \rightarrow silica-Au(OH)_2 + H_2O \quad (2)$$

$$silica-Au(OH)_2 \rightarrow silica-Au(OH) + H_2O \quad (3)$$

$$HAuCl(OH)_3 + silica \rightarrow silica-Au(OH) + 2H_2O + HCl$$
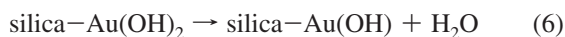$$\text{(total reaction)} \quad (4)$$

It should be noted that each intermediate species can be dehydrated without making a Au-O-Si linkage. The intermediate Au species are negatively charged similar to the precursor; therefore; in order to keep the system neutral, a charge-compensating proton is added at the opposite surface of the slab.
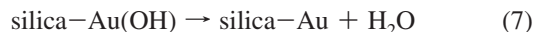
Thus, a first intermediate gives structure 3C following

$$silica-Au(OH)_3 \rightarrow silica-Au(OH)_2 + H_2O \quad (5)$$
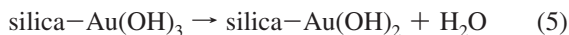
a second one gives structure 3E following

$$silica-Au(OH)_2 \rightarrow silica-Au(OH) + H_2O \quad (6)$$

and, finally, a last completely dehydrated one, structure 3F, following

$$silica-Au(OH) \rightarrow silica-Au + H_2O \quad (7)$$

(The dehydrated silanols implicated in the dehydration reactions are not included in eqs 1–7.)

To estimate the relative stability between the chemisorbed species, we use an atomistic thermodynamics approximation, as described and used with success in refs 6, 15, and 16.

We consider the gold/silica system in contact with a gaseous HCl and gaseous H_2O reservoir. From the electronic energy, the free energy of the water/HCl/gold/silica interface, under known thermodynamic conditions, may be estimated following the approximations used in our former studies,[6,15,16] as originating from Kaxiras et al.[29] and Qian et al.[30] It consists in the neglect of the variation of the chemical potentials of the surfaces with the adsorption and the consideration of the gas phase as a perfect gas. In the proposed scheme, the free energy of water and HCl (including the ZPE correction) in the gas phase is

$$\Delta G(H_2O) = E(H_2O) - ((\Delta H_G - T\Delta S_G(T)) + RT\ln(p/p°)) \quad (8)$$

$$\Delta G(HCl) = E(HCl) - ((\Delta H_G - T\Delta S_G(T)) + RT\ln(p/p°)) \quad (9)$$

where $E(H_2O)$ and $E(HCl)$ are the electronic energy of water calculated at 0 K, ΔH_G and $\Delta S_G(T)$ are the enthalpy and entropy of gaseous species, calculated with the Gaussian03 code[31] as a function of the temperature, p is the partial pressure of water vapor, and $p°$ is the standard pressure (1 bar). The minor entropy contributions to the vibrations of the surface are neglected.[32]

Using the above-mentioned formalism, the free energy of reactions 8 and 9 for the formation of the mono-, di-, and trigrafted gold complexes from the monografted one at equilibrium conditions are then expressed as

$$\Delta G_1 = E(silica-Au(OH)_3) + \Delta G(HCl) - E(HAuCl(OH)_3) - E(silica) \quad (10)$$

$$\Delta G_2 = E(silica-Au(OH)_2) + \Delta G(H_2O) - E(silica-Au(OH)_3) \quad (11)$$

$$\Delta G_3 = E(silica-Au(OH)) + \Delta G(H_2O) - E(silica-Au(OH)_2) \quad (12)$$

and similar for the second series of intermediates (eqs 5–7).

In this approximation, we consider that the energies of the mono- to di- and di- to trigrafted transitions are independent of the degree of hydration of the silica surface. It is known experimentally that silanols are stable at silica surfaces until 673 K. Above this temperature, silanols begin to condensate into siloxane bridges.[33] Thus, our model with 5.8 OH/nm^2, corresponding to conditions of a hydroxylated surface, remains valid until the temperature of 673 K.

Figure 4 shows the free energy, ΔG, of the grafted Au complexes on the silica surface as a function of temperature (T) for a water partial pressure (p) equivalent to the ambient air water partial pressure $(p_w = 1500 \text{ Pa})$.[34] From our set of structures, the most stable isomeric forms are retained to draw the phase diagram. At the above-mentioned conditions, the digrafted model (structure 3B) is the most stable until $T = 290$

Formation of Au Clusters Supported on Si Surfaces

*J. Phys. Chem. C, Vol. 114, No. 19, 2010* **9005**
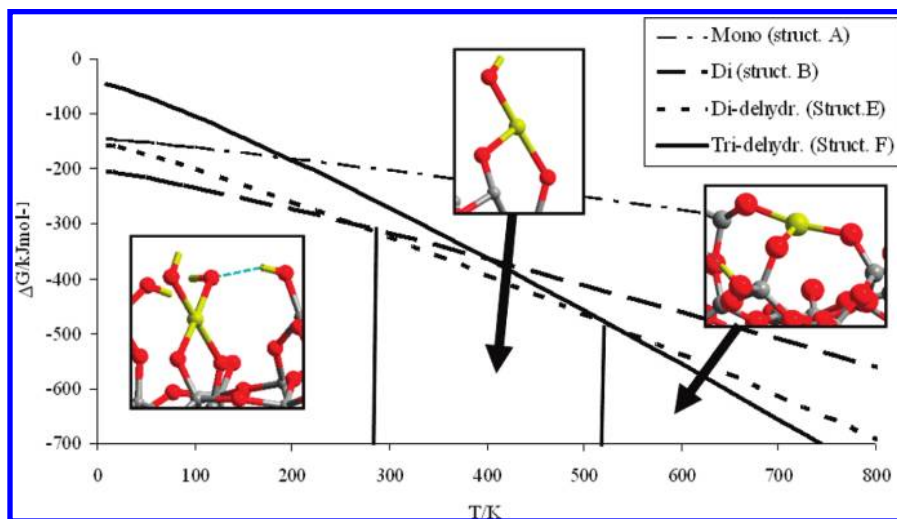
Figure 4. Phase diagram (free energy vs temperature) showing the stability ranges for the different grafting geometries.

K, followed by the digrafted dehydrated model (structure 3E) in the 290−520 K domain, and finally at $T > 520$ K, the trigrafted dehydrated model (structure 3F) is found as the most stable configuration, corresponding to a substitution of a framework $SiOH^{3+}$ by a Au^{III}. The latest result should be taken with care because our model is only justified up to 673 K due to the change in surface conditions at these temperatures.

From the thermodynamic approach, one concludes that the most stable species at low temperature is the digrafted $Au(OH)_2(O-Si)_2$ complex. This configuration corresponds to the fully hydrated gold catalyst on the silica support. An increase in temperature or a decrease in hydration stabilizes the digrafted dehydrated $Au(OH)(O-Si)_2$ complex. High temperatures favor the formation of Au framework sites.

Vibrational Frequency Analysis. After the geometry optimization, the most stable structures are selected to be analyzed on the hydroxyl vibrations, that is, the chemisorbed species (mono-, di-, and trigrafted) and two physisorbed complexes involving the precursor $Au(OH)_3Cl^-$. The terminal silanol in the digrafted gold species is chosen as a reference (silanol frequency was set to 3736 cm^{-1}).[6] This procedure corresponds in using a scaling factor equal to 0.981 for the calculation level used. When this scaling factor is used, the AuO−H vibrations are predicted to be in the interval of 3658−3610 cm^{-1}. This assumption would imply that the Si−OH and the Au−OH groups have similar bonding properties.

Experimentally, no evidence was found until now for the presence of Au−O or Au−OH species. In TOF-SIMS experiments, no such fragments were detected due to their too short life times, which is in agreement with our former theoretical predictions.[35] We decided to investigate the IR spectra carefully for the presence of Au−OH groups around 3650 cm^{-1} wavenumbers. In Figure 5, the spectra of pure ordered mesoporous silica (MCM-41) and the gold grafted one (Au/MCM-41) are compared. It is evidenced that MCM-41 exhibits only one band at 3740 cm^{-1} from silanol groups, whereas the Au grafted material shows, besides the IR band from silanol groups at 3740 cm^{-1}, also a wide tail until 3400 cm^{-1} that covers OH bands that resulted from gold introduction. It is clear that this tail includes the band at about 3650 cm^{-1} from Au−OH species, as concluded from the calculations (vide infra). Moreover, a shoulder at about 3550 cm^{-1} is well-distinguished. In the literature,[36,37] the band at ca. 3550 cm^{-1} in the ordered mesoporous silica has been assigned to geminal associated with terminal silanol groups. In the present case, one can say that
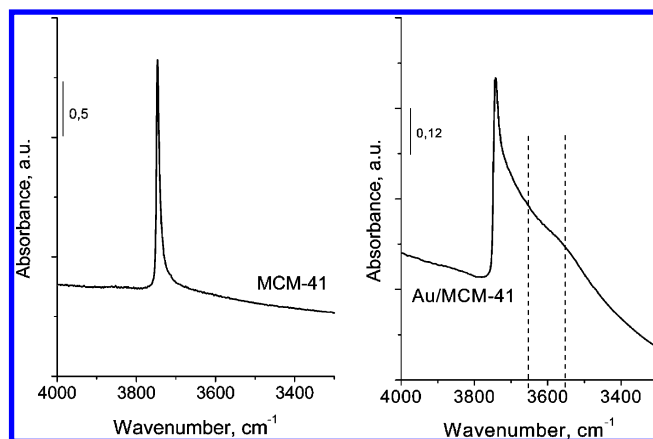
Figure 5. Experimental IR spectra of Au/MCM-41 compared with MCM-41.
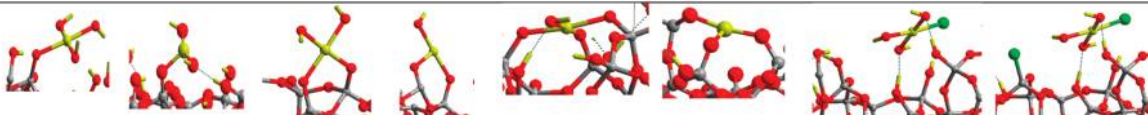
these silanol groups are not easy to remove from the MCM-41 surface when gold is present[38] (see Figure 5).

Comparing these values with our predictions, one can use these experimental values as reference for our theoretical vibration frequencies and calculate a scaling factor for the Au−OH groups, which would be more appropriate than to use the same as the one for the Si−OH groups, which are expected to be chemically different. The scaling factor used is 0.986.

When experiment and theory are compared, a first conclusion can be drawn. Namely, no or very few Au−OH groups are implicated in H-bond complexes (wavenumbers below 3630 cm^{-1}), which would exclude the presence of physisorbed precursor species. This finding brings us to the chemisorbed species as a potential anchor point or nucleation center for the gold cluster because the physisorbed precursor fragments interact much more weakly (see Table 1) with the silica surface than the precursor. The physisorbed species are probably washed away during the treatment.

Because the trigrafted species has only one Au−OH group vibrating with a specific frequency (3610 cm^{-1}), one concludes that the species responsible for the experimental IR bands are the mono- and digrafted gold species. Indeed, because the presence of these species is mainly dependent on the thermodynamic conditions, as has been shown above, the experimental vibration bands around 3650 cm^{-1} are assigned to species having structure 3B and 3E, that is, digrafted gold species.

TABLE 2: Calculated Frequencies for SiO−H and AuO−H Bond Vibrations of the Chemisorbed and Physisorbed Gold Species (in cm^{-1})

Vibration	Chem. Sorpt. Mono-grafted	Chem. Sorpt. Mono-grafted – H$_2$O	Chem. Sorpt. Di-grafted	Chem. Sorpt. Di-grafted - H$_2$O	Chem. Sorpt. Tri-grafted	Chem. Sorpt. Tri-grafted - H$_2$O (Insertion)	Phys. Sorpt. Precursor	Phys. Sorpt. Prec. + Cl-surf
Terminal SiO-H	3735		3752		3760		3735	3818
AuO-H	3658	3656	3650	3624	3610		3655	3665
	3632	3648	3619				3622	3617
	3615						3616	3597
H-bonded SiO-H	3652	3492	3613		3013		2870	2954
							2459	2443
O-Au-O						877 bend. sym. 511 bend. asym.		

Discussion and Conclusions

In this study, we investigated the effect of the cluster size and the formation of grafted gold species to the surface. Concerning the results obtained for the cluster size effect, the following can be concluded. The physisorption strength of gold on silica decreases with increasing chloride concentration at the surface, with increasing cluster size, and with decreasing oxidation state of gold. However, the gold precursor is adsorbed more strongly than the corresponding precursor fragments and this via an H-bond network.

Concerning the chemisorbed species, we found that the three grafted species studied may exist on a silica surface, depending on the experimental conditions. In dehydrated conditions (high temperatures, low partial pressures), the framework Au^{III} centers are stabilized, whereas in hydrated conditions (low temperatures, high water pressures), the dihydroxylated species Au(OH)$_2$-(O−Si)$_2$ is predominant, passing via the monohydroxylated digrafted species Au(OH)(O−Si)$_2$. They are supposed to reversibly interconvert in the presence of water and thus coexist at the surface.

It is interesting to note that the geometry of the most stable gold atom complexes is planar, in agreement with the planar geometry of the Au$_n$ ($n < 8$) gas-phase gold clusters.[14]

From the vibrational frequencies and especially by the presence of bands at 3650 cm^{-1}, it is concluded that the gold species after calcination are probably present under the form of digrafted chemisorbed species, dependent on the degree of hydration.

This information enables us to propose a possible scenario for the formation of gold clusters at the silica surface, and it is as follows: The commonly used gold precursor (HAu(OH)$_3$Cl) physisorbes at the silica surface via a H-bond network. The adsorption complex is very sensitive to the presence of chloride at the surface. After calcination, this complex generates mono- or/and digrafted gold species (preferably digrafted), which are the nucleation centers of the gold clusters.

One can speculate that these centers might attract mobile gold atoms or precursor fragments (AuCl, AuOH, etc.) through aurophilic interactions, leading to the formation of gold clusters containing different hundreds of atoms. At the surface of these clusters, one might encounter some leftovers of the precursor, such as hydroxyl and chloride groups. These groups will determine the final oxidation state of the cluster, being between +1 and 0, or the oxidation state of a particular area of the cluster. The presence of these chloride and hydroxyl groups, which might also explain the reactivity of gold nanoclusters, points into the direction of the double affinity to reactants, in the sense that, for the oxidation of CO, the oxygen molecule and the CO molecule adsorb at different sites on the catalyst,[35] that is, one molecule in the neighborhood of the chloride and hydroxyl groups, while the other prefers the metallic gold area of the cluster.

This cluster formation scenario can be used to explain the improvement of the dispersion in the recently characterized group V doped silica materials used as a support for the gold clusters.[39] The group V atoms act as "more efficient than gold itself" nucleation centers for gold, similar as is expected for the chemisorbed gold atoms on the silica surface.

References and Notes

(1) Bond, G. C.; Louis, C.; Thompson, D. T. *Catalysis by Gold*; Imperial College Press: London, 2006.

(2) Sobczak, I.; Kusior, A.; Grams, J.; Ziolek, M. *J. Catal.* **2007**, *245*, 259.

(3) Zhuravlev, L. T. *Langmuir* **1987**, *3*, 316.

(4) Wojtaszek, A.; Sobczak, I.; Ziolek, M.; Tielens, F. *J. Phys. Chem. C* **2009**, *113*, 13855.

(5) Tielens, F.; Gervais, C.; Lambert, J.-F.; Mauri, F.; Costa, D. *Chem. Mater.* **2008**, *20*, 3336.

(6) Islam, M. M.; Costa, D.; Calatayud, M.; Tielens, F. *J. Phys. Chem. C* **2009**, *113*, 10740.

(7) Costa, D.; Tougerti, A.; Tielens, F.; Gervais, C.; Mauri, F.; Stievano, L.; Lambert, J.-F. *Phys. Chem. Chem. Phys.* **2008**, *42*, 6360.

(8) Costa, D.; Tielens, F.; Stievano, F.; Lambert, J.-F. Theory and Applications of Computational Chemistry - 2008. *AIP Conference Proceedings*; 2009; Vol. 1102, pp 251−256.

(9) Nechayev, Y. A.; Zvonareva, G. V. *Geokhimiya* **1983**, *6*, 919.

(10) Moreau, F.; Bond, G. C.; Taylor, A. O. *J. Catal.* **2005**, *231*, 105.

(11) Sobczak, I. *Catal. Today* **2009**, *142*, 258.

(12) Zhuravlev, L. T. *Colloids Surf.* **2000**, *A173*, 1.

(13) Yoon, B.; Häkkinen, H.; Landman, U. *J. Phys. Chem. A* **2003**, *107*, 4066.

(14) Olson, R. M.; Varganov, S.; Gordon, M. S.; Metiu, H.; Chretien, S.; Piecuch, P.; Kowalski, K.; Kurcharski, S. A.; Musial, M. *J. Am. Chem. Soc.* **2005**, *127*, 1049.

(15) Tielens, F.; Calatayud, M.; Franco, R.; Recio, J. M.; Minot, C.; Perez-Ramirez, J. *Solid State Ionics* **2009**, *180*, 1011.

(16) Tielens, F.; Humblot, V.; Pradier, C.-M.; Calatayud, M.; Illas, F. *Langmuir* **2009**, *25*, 9980.

(17) Kresse, G.; Furthmuller, J. *Phys. Rev. B* **1996**, *54*, 11169.
(18) Kresse, G.; Joubert, J. *Phys. Rev. B* **1999**, *59*, 1758.
(19) Perdew, J. P.; Burke, K.; Ernzerhof, M. *Phys. Rev. Lett.* **1996**, *77*, 3865.
(20) Perdew, J. P.; Burke, K.; Ernzerhof, M. *Phys. Rev. Lett.* **1997**, *78*, 1396.
(21) Zhang, Y. K.; Yang, W. T. *Phys. Rev. Lett.* **1998**, *80*, 890.
(22) Gu, X.; Ji, M.; Wei, S. H.; Gong, X. G. *Phys. Rev. B* **2004**, *70*, 205401.
(23) Tielens, F.; Andrés, J.; Van Brussel, M.; Buess-Herman, C.; Geerlings, P. *J. Phys. Chem. B* **2005**, *109*, 7624.
(24) Tielens, F.; Andrés, J. *J. Phys. Chem. C* **2007**, *111*, 10342.
(25) Tielens, F.; Andrés, J.; Chau, T.-D.; de Bocarmé, T. V.; Kruse, N.; Geerlings, P. *Chem. Phys. Lett.* **2006**, *421*, 433.
(26) de Bocarmé, T. V.; Chau, T.-D.; Tielens, F.; Andrés, J.; Gaspard, P.; Wang, L. R. C.; Kreuzer, H. J.; Kruse, N. *J. Chem. Phys.* **2006**, *125*, 054703.
(27) Blöchl, P. E. *Phys. Rev. B* **1994**, *50*, 17953.
(28) Kresse, G.; Joubert, J. *Phys. Rev. B* **1999**, *59*, 1758.
(29) Kaxiras, E.; Bar-Yam, Y.; Joannopoulos, J. D.; Pandey, K. C. *Phys. Rev. B* **1987**, *35*, 9625.
(30) Qian, G. X.; Martin, R. M.; Chadi, D. J. *Phys. Rev. B* **1988**, *38*, 7649.
(31) Frisch, M. J.; Trucks, G. W.; Schlegel, H. B.; Scuseria, G. E.; Robb, M. A.; Cheeseman, J. R.; Montgomery, J. J. A.; Vreven, T.; Kudin, K. N.; Burant, J. C.; Millam, J. M.; Iyengar, S. S.; Tomasi, J.; Barone, V.; Mennucci, B.; Cossi, M.; Scalmani, G.; Rega, N.; Petersson, G. A.; Nakatsuji, H.; Hada, M.; Ehara, M.; Toyota, K.; Fukuda, R.; Hasegawa, J.; Ishida, M.; Nakajima, T.; Honda, Y.; Kitao, O.; Nakai, H.; Klene, M.; Li, X.; Knox, J. E.; Hratchian, H. P.; Cross, J. B.; Bakken, V.; Adamo, C.; Jaramillo, J.; Gomperts, R.; Stratmann, R. E.; Yazyev, O.; Austin, A. J.; Cammi, R.; Pomelli, C.; Ochterski, J. W.; Ayala, P. Y.; Morokuma, K.; Voth, G. A.; Salvador, P.; Dannenberg, J. J.; Zakrzewski, V. G.; Dapprich, S.; Daniels, A. D.; Strain, M. C.; Farkas, O.; Malick, D. K.; Rabuck, A. D.; Raghavachari, K.; Foresman, J. B.; Ortiz, J. V.; Cui, Q.; Baboul, A. G.; Clifford, S.; Cioslowski, J.; Stefanov, B. B.; Liu, G.; Liashenko, A.; Piskorz, P.; Komaromi, I.; Martin, R. L.; Fox, D. J.; Keith, T.; Al-Laham, M. A.; Peng, C. Y.; Nanayakkara, A.; Challacombe, M.; Gill, P. M. W.; Johnson, B.; Chen, W.; Wong, M. W.; Gonzalez, C.; Pople, J. A. *Gaussian 03*, revision C.02; Gaussian, Inc.: Wallingford, CT, 2004.
(32) Reuter, K.; Scheffler, M. *Phys. Rev. B* **2001**, *65*, 035406.
(33) Bolis, V.; Fubini, B.; Marchese, L.; Martra, G.; Costa, D. *J. Chem. Soc., Faraday Trans.* **1991**, *87*, 497.
(34) Guyot, A.; Curtis, G. E.; Libbey, W. *Smithsonian Meteorological Tables: Based on Guyot's Meteorological and Physical Tables*; 1896.
(35) Tielens, F.; Gracia, L.; Polo, V.; Andrés, J. *J. Phys. Chem. A* **2007**, *111*, 13255.
(36) Berndt, H.; Martin, A.; Brückner, A.; Schreier, E.; Müller, D.; Kosslick, H.; Wolf, G.-U.; Lücke, B. *J. Catal.* **2000**, *191*, 384.
(37) Zhou, R.; Cao, Y.; Yan, S.; Deng, J.; Liao, Y.; Hong, B. *Catal. Lett.* **2001**, *75*, 107.
(38) Ryczkowski, J.; Goworek, J.; Gac, W.; Pasieczna, S.; Borowiecki, T. *Thermochim. Acta* **2005**, *434*, 2.
(39) Sobczak, I.; Kieronczyk, N.; Trejda, M.; Ziolek, M. *Catal. Today* **2008**, *139*, 188.